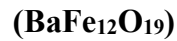


# Effect of Grain Size on Electric and Magnetic Properties of Barium Hexaferrite



R. Pattanayak, N.Parween, P Sahu, S.Rout, R.Mudulli & S.Panigrahi

Department of Physics and Astronomy, National Institute of Technology Rourkela , 769008,

India

Polycrystalline Barium hexaferrite (BaFe<sub>12</sub>O<sub>19</sub>) having variable grain sizes were prepared by auto-combustion and solid state technique. SEM micrograph shows the variation of grain size (from nano range to bulk) of the system prepared at different temperatures. For this work electric transport (in the frequency range 100Hz to 1Mz) and magnetic study (M-H loop) carried out at room temperature. From the electric study it was found that, resistivity of the system varies inversely with grain size, however saturation magnetization ( $M_s$ ) varies directly with grain size. In our report we were attempted to resolve the relation between grain size with electric and magnetic properties of the studied system.

Keywords: Microstructure, Impedance, Modulus, Magnetization

## 1. Introduction:

Barium hexaferrite (BaFe<sub>12</sub>O<sub>19</sub>) is widely used as a permanent magnet material as it possesses large saturation magnetization ( $M_s$ ), high coercive force ( $H_c$ ) and high magnetic anisotropy ( $H_a$ ) along with excellent chemical stability and corrosion resistivity [1–4]. Apart from large scale applications in permanent magnets such as: motors, actuators, sensors, isolators, circulators, phase shifters, and miniature antennas etc., its ultrafine particle is distinctly used for high density recording media to increase the storage capacity and reduce medium noise [5,6]. BaM system retains hexagonal structure consists of a close-packed stacking of oxygen layers, with the iron (Fe) atoms distributed within three kinds of octahedral sites (12k, 2a and 4f<sub>2</sub>), one tetrahedral site (4f<sub>1</sub>), and one bi-pyramidal site (2b) which are coupled by super exchange interactions through the O<sup>2-</sup> ions [12]. The magnetic and electrical properties of the BaM system depend on the distribution of the cations in octahedral, tetrahedral and bi-pyramidal sites [12-21].

## 2. Experimental Techniques:

Barium hexaferrite nano range particles were prepared by the auto combustion method. Analytical grades Iron Nitrate  $\text{Fe}(\text{NO}_3)_3 \cdot 9\text{H}_2\text{O}$  and Barium Nitrate  $\text{Ba}(\text{NO}_3)_2$  were taken as oxidants where Glycine ( $\text{C}_2\text{H}_5\text{NO}_2$ ) used as fuel for combustion. The stoichiometric amounts of these nitrates dissolved in distilled water and stirred at  $150^\circ\text{C}$  for for proper homogenous mixture. After 2-3h stirring all the water evaporates and combustion taken place. Finally brown like powder was collected. The powder was calcined at  $900^\circ\text{C}$  for 12h and then formation of BaM pure phase was confirmed by the Rigaku Ultima-IV X-ray diffractometer (Cu target). For electric study the calcinated powder pressed into cylindrical pellets and sintered at  $950^\circ\text{C}$  for 5h then pure phase formation of BaM confirmed by X-ray diffractometer. For increasing of grain size we sinter the same pellet at  $1000^\circ\text{C}$  for 5h and  $1100^\circ\text{C}$  for 3h. The surface morphology of the BaM nanoparticle was estimated by the Nova Nano SEM-450 Field emission scanning electron microscopy (FESEM). Room temperature impedance with respect to frequency was measured by using HIOKI impedance analyzer (model IM3570) from 100 Hz to 1 MHz. The room temperature M-H loop study for all the systems done by SQUID VSM (Quantum Design).

### 3. Result and Discussion

#### 3.1 Structural and Microstructural Study:

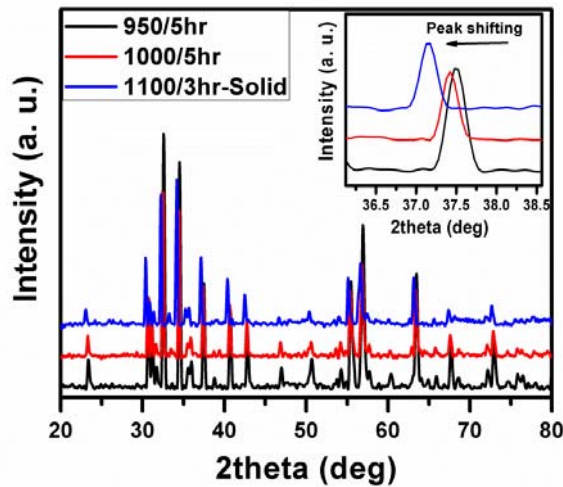


Fig.1

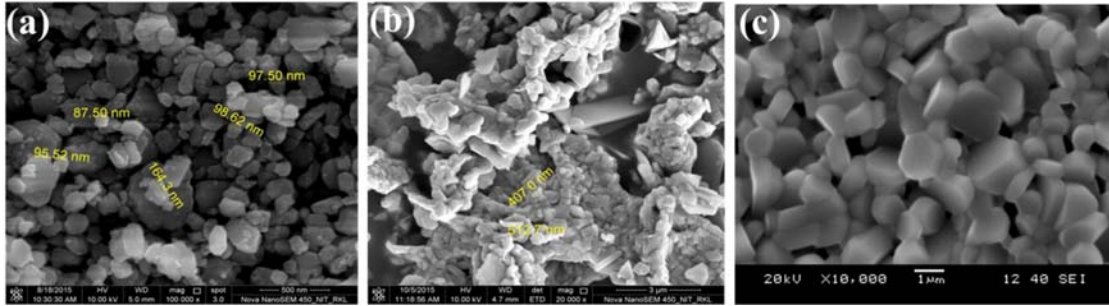


Fig. 2

From the Fig. 1 it was confirmed that all the X-ray diffraction peaks are matched with pure phase of BaM system without appearing of any extra peak. We can also observe that (insight of Fig. 1) peak shifts towards left with rise of temperature which is the indication of increasing of grain growth. From SEM micrograph it was well observed that the grains densely packed inside the system. It was also confirmed that grain size increases from nano range to micro range as the sintering temperature increases. Here Fig. 2a, 2b and 2c sintered at 950°C, 1000°C and 1100°C respectively.

### 3.2 Impedance and Modulus Study:

From the Fig. it was observed that as grain size increases the resistive part ( $Z'$ ) of systems decreases. Here we can expect that, increasing of grain size can reduce the grain boundary density for a system which has higher resistive nature than grain hence resistance of the system reduced. From the reactive nature ( $Z''$ ) of the systems we can predict that all the systems have relaxation behaviour at room temperature. But quantitatively, the behaviour of  $Z'$  and  $Z''$  with frequency are not exactly same. For examine the intrinsic and extrinsic contribution of the relaxation behaviour we taken the help of cole-cole of impedance and modulus spectroscopic study.

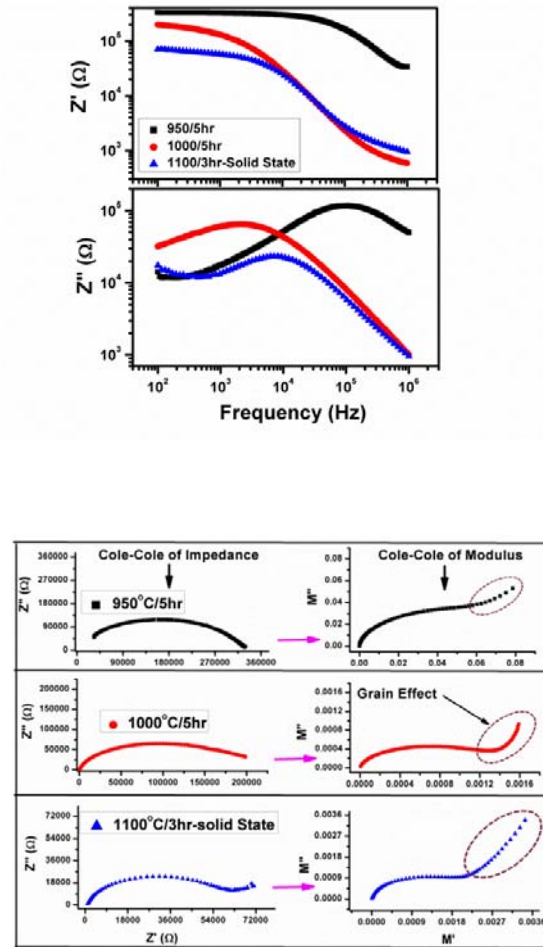


Fig. shows the cole-cole impedance and modulus at room temperature (RT). The cole-cole of impedance graph single relaxation behaviour due to which only single semicircle appears in the graph. Pattanayk et.al worked on bulk BaM system and found co-contribution of grain and grain boundary relaxation effect at RT which was confirmed from cole-cole of modulus study. Here if we observe the cole-cole of modulus spectrum of bulk BaM system (which is fired at 1100°C) then we then we can find similar type of behaviour (i.e. a semicircle connected with a larger tail). So the tail like feature (circular mark in the figure) in the graph is the intrinsic contribution (grain) where the semicircle is due to extrinsic (grain boundary) relaxation behaviour. But it is interesting that, when the grain size reduces (i.e. sample prepared at low temperature) the tail like feature (grain effect) gradually disappears. So here we predict that as grain size reduces the short range hopping conduction dominates over long range conduction inside the grain may due to increasing of hopping distance.

### 3.3 Magnetic Study:

Fig. 12 shows the hysteresis (M– H) loops of all systems at room temperature. It can be observe that the saturation magnetization (Ms), remnant magnetization (Mr) and coercive field (Hc) increases with rise of temperature (values are given in Table 4 ). The saturation magnetization of samples is derived from the law of saturation using the following equation (2) [i]:

$$M = M_s \left( 1 - \frac{A}{H} - \frac{B}{H^2} \right) + \chi_p H \dots\dots\dots(2)$$

Where  $M_s$  is the saturation magnetization, A is inhomogeneity parameter,  $\chi_p$  is the high field susceptibility and B is the anisotropy parameter. For hexagonal crystal structure, B can be expressed as equation (3):

$$B = \frac{H_a^2}{15} = \frac{4K_1^2}{15M_s^2} \dots\dots\dots(3)$$

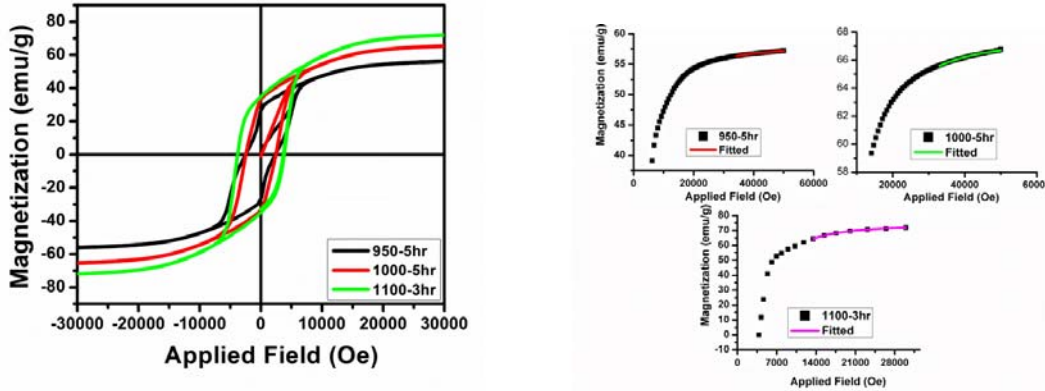
Where  $H_a$  is anisotropy field and  $K_1$  is magneto-crystalline anisotropy constant (**intrinsic magnetic parameter**). The magneto-crystalline anisotropy constant can be **calculate from** quantitative analyses of the M-H curve by using the law of approach to saturation (LAS). The LAS can be written as (equation 4) [ii]:

$$M = M_s \left( 1 - \frac{8K_1^2}{105\mu_0^2 M_s^2 H^2} \right) + cH \dots\dots\dots(4)$$

$M_s$  is the saturation magnetization,  $\mu_0$  is the magnetic permeability in free space, and c is linear constant term. The phenomenological linear term cH is very small at high magnetic field. The M-H loop was fitted (insights of Fig. 9) by using the equation (4) and magneto-crystalline anisotropy constants ( $K_1$ ) were estimated (Table 3). Then anisotropy field ( $H_a$ ) values were for both the system calculated by using equation 3.

It was observed that (Table 3) for composite system  $H_a$  was reduced as compared with BaM system. From the above discussion it can be predict that, presences of BaM-NBT interfaces in the system pinning of magnetization at the grain boundaries as the result anisotropy field

reduced. When the anisotropy field reduced it lowers the activation energy barrier by which domain walls will free to move hence coercivity of the composite system reduced [41].



Parameters → Compositions ↓	$M_s$ (emu/g)	$M_r$ (emu/g)	$H_c$ (Oe)	Anisotropy Constant ( $K_1$ ) (erg/cm <sup>3</sup> )	$H_a$ (kOe)
950-5hr	57	29	2425	1.19E6	41.75
1000-5hr	67	33	2598	1.38E6	41.19
1100-3hr	73	34	3811	1.21E6	33.61

From Table- it can be observed that the saturation magnetization increases with grain size which may be due to larger domain size (decreasing of domain density) with less random orientation having less anisotropic field ( $H_a$ ). But here we observe a contradictory result that with decreasing of  $H_a$  increasing of  $H_c$ . It was well known that if  $H_a$  reduces the domain wall strength will be reduced which can help to easy rotation of domain along the field direction.

#### 4. Conclusion:

Polycrystalline Barium hexaferrite ( $BaFe_{12}O_{19}$ ) having variable grain sizes were prepared by using auto-combustion and solid state technique. SEM micrograph shows the variation of grain size (from nano range to bulk) of the system prepared at different temperatures. From the complex impedance spectroscopy it was found that grain relaxation evolves when the grain size of system increase. From magnetic study (M-H loop) it was found that as grain size increase the saturation magnetization increases.

#### Acknowledgment:

The authors want to acknowledge Prof. D. Behera, Department of Physics and Astronomy, NIT Rourkela for valuable discussions. To Biswanath Samantaray, Saha Institute of Nuclear Physics, 1/A Bidhannagar, Calcutta - 700064, India, for collection of magnetic data and Ministry of Human Resource Development (MHRD), Government of India for providing scholarship.

### **References:**

- [1] S. Castro, M.G. Rivas, J.M. Greneche, J. Mira, C. Rodrlguez, *Journal of Magnetism and Magnetic Material* 152 (1996) 61–69.
- [2] A. Mali, A. Ataie, *Scripta Mater.* 53 (2005) 1065.
- [3] Vivek A. Rane, Sher Singh Meena, Suresh P. Gokhale, S.M. Yusuf, Girish J. Phatak, and Sadgopal. Date, *Journal of Electronic Materials*, 42 (2013) 4.
- [4] Y.Y. Meng, M.H. He, Q. Zeng, D.L. Jiao, S. Shukla, R.V. Ramanujan, Z.W. Liu, *Journal of Alloys and Compounds* 583 (2014) 220–225.
- [5] T. Fujiwara, *IEEE Transactions* 21 (1985) 1480–1485.
- [6] K. Yamamori, T. Suzuki, T.M. Fujiwara, *IEEE Transactions* 22 (1986) 1188–1190.
- [12] F. M. M. Pereira, C. A. R. Junior, M. R. P. Santos, R. S. T. M. Sohn, F. N. A. Freire, J. M. Sasaki, J. A. C. de Paiva, A. S. B. Sombra, *J Mater Sci: Mater Electron*, 19 (2008) 627–638.
- [13] H. S ozeri, I. Kucuk, H. O zkan, *Journal of Magnetism and Magnetic Materials* 323 (2011) 1799–1804.
- [14] S.M. El-Sayed a,n, T.M. Meaz b,1, M.A. Amer b,2, H.A. El Shersaby, *Physica B* 426 (2013) 137–143.
- [15] Cong-Ju Li, BinWang, Jiao-NaWang, *Journal of Magnetism and Magnetic Materials* 324 (2012) 1305–1311.
- [16] Sonal Singhal, Tsering Namgyal, Jagdish Singh, Kailash Chandra, Sandeep Bansal, *Ceramics International* 37 (2011) 1833–1837.

- [17] Ashima, Sujata Sanghi, Ashish Agarwal, Reetu, Journal of Alloys and Compounds 513 (2012) 436– 444.
- [18] Daming Chen, Yingli Liu, Yuanxun Li, Kai Yang, Huaiwu Zhang, Journal of Magnetism and Magnetic Materials 337–338 (2013) 65–69.
- [19] A. Haq, M. Anis-ur-Rehman, Physica B 407 (2012) 822–826.
- [20] Vaishali V. Soman, V.M. Nanoti, D.K. Kulkarni, Ceramics International 39 (2013) 5713–5723.
- [21] H. Sözeri, H. Deligöz, H. Kavas, A. Baykal, Ceramics International 40 (2014) 8645–8657.
- [22] Ashima, Sujata Sanghi, Ashish Agarwal, Reetu, Neetu Ahlawat, J. Appl. Phys. 112 (2012) 014110.

---

[i] Grössinger R. J Magn Magn Mater, 28 (1982) 137.

[ii] S. Chikazumi, Physics of Ferromagnetism, 2nd ed. (Oxford University Press, Oxford, 1997).

[41] B.K.Bammannavar,L.R.Naik,J. Magn.Magn.Mater.321(2009)382-387.

[7] [A.N.Bogdanov & I.E.Dragunov 1998](#)